Diabetologia (2016) 59:614–623
DOI 10.1007/s00125-015-3829-8

ARTICLE

Disruption of calcium transfer from ER to mitochondria links alterations of mitochondria-associated ER membrane integrity to hepatic insulin resistance

Jennifer Rieusset[1] · Jeremy Fauconnier[2] · Melanie Paillard[1] · Elise Belaidi[1] · Emily Tubbs[1] · Marie-Agnès Chauvin[1] · Annie Durand[1] · Amélie Bravard[1] · Geoffrey Teixeira[1] · Birke Bartosch[3] · Maud Michelet[3] · Pierre Theurey[1] · Guillaume Vial[1] · Marie Demion[2] · Emilie Blond[1,4] · Fabien Zoulim[3,4] · Ludovic Gomez[1] · Hubert Vidal[1] · Alain Lacampagne[2] · Michel Ovize[1,4]

Received: 25 June 2015 / Accepted: 17 November 2015 / Published online: 10 December 2015

Abstract
Aims/hypothesis Mitochondria-associated endoplasmic reticulum membranes (MAMs) are regions of the endoplasmic reticulum (ER) tethered to mitochondria and controlling calcium (Ca^{2+}) transfer between both organelles through the complex formed between the voltage-dependent anion channel, glucose-regulated protein 75 and inositol 1,4,5-triphosphate receptor (IP3R). We recently identified cyclophilin D (CYPD) as a new partner of this complex and demonstrated a new role for MAMs in the control of insulin's action in the liver. Here, we report on the mechanisms by which disruption of MAM integrity induces hepatic insulin resistance in *CypD* (also known as *Ppif*)-knockout (KO) mice.
Methods We used either in vitro pharmacological and genetic inhibition of CYPD in HuH7 cells or in vivo loss of CYPD in mice to investigate ER–mitochondria interactions, inter-organelle Ca^{2+} exchange, organelle homeostasis and insulin action.
Results Pharmacological and genetic inhibition of CYPD concomitantly reduced ER–mitochondria interactions, inhibited inter-organelle Ca^{2+} exchange, induced ER stress and altered insulin signalling in HuH7 cells. In addition, histamine-stimulated Ca^{2+} transfer from ER to mitochondria was blunted in isolated hepatocytes of *CypD*-KO mice and this was associated with an increase in ER calcium store. Interestingly, disruption of inter-organelle Ca^{2+} transfer was associated with ER stress, mitochondrial dysfunction, lipid accumulation, activation of c-Jun N-terminal kinase (JNK) and protein kinase C (PKC)ε and insulin resistance in liver of *CypD*-KO mice. Finally, CYPD-related alterations of insulin signalling were mediated by activation of PKCε rather than JNK in HuH7 cells.
Conclusions/interpretation Disruption of IP3R-mediated Ca^{2+} signalling in the liver of *CypD*-KO mice leads to hepatic insulin resistance through disruption of organelle interaction and function, increase in lipid accumulation and activation of PKCε. Modulation of ER–mitochondria Ca^{2+} exchange may thus provide an exciting new avenue for treating hepatic insulin resistance.

Keywords Calcium signalling · Cyclophilin D · Endoplasmic reticulum · Inositol 1,4,5-triphosphate receptor · Insulin resistance · Liver · Mitochondria · Mitochondria-associated endoplasmic reticulum membranes · PKCε

Jeremy Fauconnier and Melanie Paillard contributed equally to this work.

An earlier version of this paper was published in *Hepatology* in 2013 but was retracted after errors in the presentation of western blot data became apparent (DOI: 10.1002/hep.26189). At the authors' request their institutions (Research Offices of Inserm, Lyon and Montpellier Universities) checked the integrity of all the raw data, concluding that the mistakes that led to the retraction were a result of honest error.
The images presented here have all passed image forensics screening.

Electronic supplementary material The online version of this article (doi:10.1007/s00125-015-3829-8) contains peer-reviewed but unedited supplementary material, which is available to authorised users.

✉ Jennifer Rieusset
jennifer.rieusset@univ-lyon1.fr

[1] Inserm UMR-1060, Laboratoire CarMeN, Université Lyon 1, 165 chemin du grand Revoyet, BP12, 69921 Oullins cedex, France

[2] Inserm U1046-CNRS UMR-9214, PhyMedExp, Université Montpellier, Montpellier, France

[3] Inserm UMR-1052, Centre de recherche en Cancérologie de Lyon, Université Lyon 1, Lyon, France

[4] Hospices Civils de Lyon, Lyon, France

Abbreviations

CsA	Ciclosporin (cyclosporin A)
CYPD	Cyclophilin D
DAG	Diacylglycerol
EIF2α	Eukaryotic translation initiation factor 2α
ER	Endoplasmic reticulum
GRP75	Glucose-regulated protein 75
IP3R	Inositol 1,4,5-triphosphate receptor
JNK	c-Jun N-terminal kinase
KO	Knock-out
MAM	Mitochondrial-associated endoplasmic reticulum membrane
MFN2	Mitofusin 2
PKB	Protein kinase B
PKCε	Protein kinase C epsilon
PLA	Proximity ligation assay
PTP	Permeability transition pore
SERCA2	Sarco(endo)plasmic reticulum Ca^{2+} ATPase 2
siRNA	Small interfering RNA
TG	Triacylglycerol
VDAC	Voltage-dependent anion channel
WT	Wild-type

Introduction

Mitochondria and endoplasmic reticulum (ER) are organised as a network with specific contact points, referred to as mitochondrial-associated ER membranes (MAMs), which play a pivotal role in calcium (Ca^{2+}) signalling and energy metabolism [1]. Efficient Ca^{2+} transmission from the ER to mitochondria is mediated through the interaction of the voltage-dependent anion channel (VDAC) of the outer mitochondrial membrane with the inositol-1,4,5-triphosphate receptor (IP3R) on the ER via the chaperone glucose-regulated protein 75 (GRP75) [2]. Mitochondrial Ca^{2+} uptake is essential for the regulation of both mitochondrial metabolism and ER homeostasis [3], and alteration of ER–mitochondria cross-talk may result in a disruption of inter-organelle Ca^{2+} transfer [4] and subsequent ER stress [5]. Under certain conditions excessive Ca^{2+} entry into the mitochondrial matrix may be detrimental, causing the opening of the permeability transition pore (PTP) and cell death [6]. Therefore, tight control of Ca^{2+} exchange between ER and mitochondria is required to regulate vital functions and metabolic homeostasis.

The molecular and functional characterisation of MAMs in physiological and pathological conditions has improved in the last few years, highlighting unexpected roles for MAMs in cellular signalling [7]. Particularly, we recently demonstrated that cyclophilin D (CYPD), a mitochondrial protein known to modulate the opening of the PTP [8], also interacts with the VDAC–GRP75–IP3R complex at the MAM interface in both heart [9] and liver [10]. In cardiomyocytes, we found that the loss of CYPD reduced mitochondrial Ca^{2+} overload by depressing ER–mitochondria interactions and protected cells against lethal reperfusion injury [9], suggesting that CYPD regulates Ca^{2+} transfer from ER to mitochondria. In liver, the loss of CYPD reduced organelle interactions and induced hepatic insulin resistance, pointing to a new role of MAM integrity in the control of insulin's action [10]. Whereas other studies in mice also suggest a role for MAMs in the control of glucose homeostasis [11–14], the mechanisms by which disruption of MAMs alters insulin signalling are unknown.

Based on the role of MAMs in Ca^{2+} transfer from ER to mitochondria, we hypothesised that a disruption of Ca^{2+} transfer between both organelles could contribute to hepatic insulin resistance. To this aim, using pharmacological and genetic loss of function approaches both in vivo and in vitro, we investigated whether the disruption of Ca^{2+} transfer from ER to mitochondria could link MAM alterations to hepatic insulin resistance in *CypD* (also known as *Ppif*)-knockout (KO) mice.

Methods

Cell culture HuH7 cells were a gift from G. Mithieux's laboratory (Inserm U855, Lyon, France) and were free of mycoplasma. They were cultured as previously described [10] and stimulated either with CYPD (ciclosporin [cyclosporin A, CsA] or NIM811) or with IP3R (2-APB and Xestospongin C) pharmacological inhibitors. Inhibition of CYPD was also achieved by silencing of *CYPD*. See electronic supplementary material (ESM) Methods for further details. For measurement of insulin signalling, cells were depleted in serum for 3 h before incubation with insulin (10^{-7} mol/l, 15 min).

Animals CYPD-KO mice on a C57Bl/6/SV129 genetic background were a gift from S. J. Korsmeyer's laboratory (Boston, MA, USA) [15]. Both male wild-type (WT) and CYPD-KO mice were obtained by homozygous intercross in our laboratory. All experiments were performed on mice of 18–22 weeks of age, and were conducted in accordance with institutional guidelines for the care and use of laboratory animals, and a regional ethics committee has approved all procedures. No randomisation or blinding were performed. No data samples or animals were excluded from the study.

Ca^{2+} measurements Using confocal fluorescence imaging, we evaluated variations in the time course of mitochondrial Ca^{2+} content simultaneously with intra-ER Ca^{2+} in a native cell environment in the presence of extracellular calcium (1.8 mmol/l $CaCl_2$) [16]. To measure mitochondrial Ca^{2+}, cells were loaded with Rhod-2 AM (3 μmol/l) whereas the measurement of ER Ca^{2+} was performed using a low-affinity Ca^{2+} indicator, Fluo-5N (5 μmol/l; ThermoFisher Scientific, MA, USA). For measurement of absolute cytosolic Ca^{2+}

levels, cells were loaded with 1 μmol/l of Fura2-AM and pluronic acid (both from ThermoFisher Scientific). See ESM Methods for further details.

ER–mitochondria interactions ER–mitochondria interactions were measured both by subcellular fractionation and by in situ proximity ligation assay (PLA), as previously described and thoroughly validated [10]. See ESM Methods for further details.

Real-time PCR mRNA levels were measured by real-time RT-PCR. See ESM Methods for further details.

Western blotting Protein expression was analysed by SDS-PAGE. See ESM Methods for further details.

Hyperinsulinaemic–euglycaemic clamp Insulin sensitivity of mice was measured during a hyperinsulinaemic–euglycaemic clamp. See ESM Methods for further details.

Primary hepatocytes Primary mouse hepatocytes were isolated via a modified collagenase perfusion method, as described previously [17]. See ESM Methods for further details.

Mitochondrial respiration Mitochondrial respiration was measured in intact or permeabilised primary hepatocytes. See ESM Methods for further details.

Hepatic lipid content Hepatic triacylglycerol (TG) and diacylglycerol (DAG) content were measured by spectrophotometry. See ESM Methods for further details.

PKCε activity PKCε activity in liver was determined by western blot based on the membrane translocation. See ESM Methods for further details.

Statistical analysis Results are expressed as mean ± SEM. Student's *t*-test was used to analyse the difference between control and experimental groups. Statistically significant differences were assessed with a one-way ANOVA with a Newman–Keuls post hoc test when three or more groups were compared. A p value <0.05 was considered as statistically significant.

Results

Pharmacological and genetic inhibition of CYPD inhibits Ca^{2+} transfer from ER to mitochondria in HuH7 cells We recently demonstrated by in situ PLA that CYPD interacted with the VDAC1–GRP75–IP3R1 calcium-channelling complex [9, 10]. Here, we challenged the interactions of CYPD with this complex using pharmacological and genetic loss of function studies, and investigated the repercussions on both ER–mitochondria interactions and Ca^{2+} transfer. As CYPD inhibitors we used CsA and NIM811 (a CsA derivative devoid of immunosuppressive activity), which are both known to detach CYPD from the inner mitochondrial membrane [18]. Treatment of HuH7 cells with CsA or NIM811 significantly inhibited CYPD–IP3R1 interactions (Fig. 1a). Reduction of CYPD expression using specific small interfering RNA (siRNA) (Fig. 1b) also significantly decreased the interactions between CYPD and IP3R1 (Fig. 1c).

Using organelle-targeted fluorescent dye, we then measured Ca^{2+} flux in HuH7 cells under histamine stimulation (100 μmol/l). Histamine binding to its receptor induces inositol-1,4,5-triphosphate elevation and activates IP3R, causing Ca^{2+} release from ER stores. Specificity and non-overlapping of the Ca^{2+}-sensitive dyes is illustrated in ESM Fig. 1. Histamine application rapidly reduced ER Ca^{2+} stores (Fig. 2a) and simultaneously increased mitochondrial Ca^{2+} content (Fig. 2b), illustrating transfer of Ca^{2+} from the ER to the mitochondria. Importantly, after NIM811 treatment or CYPD silencing, histamine was unable to induce Ca^{2+} transfer from ER to mitochondria, as illustrated by the absence of mitochondrial Ca^{2+} accumulation in both situations (Fig. 2a, b).

Inhibition of CYPD function induces ER stress and alters insulin response in HuH7 cells Next, we measured the consequences of CYPD inhibition on both ER and mitochondrial homeostasis and on insulin signalling in HuH7 cells. NIM811 treatment significantly increased mRNA levels of *GRP78*, *XBP1S* and *CHOP* (also known as *DDIT3*) (Fig. 3a), as well as the protein level of GRP78 and the phosphorylation of eukaryotic translation initiation factor 2α (EIF2α) (Fig. 3b), indicative of ER stress. However, this treatment had no effect on the mRNA levels of *HSP10* and *HSP60* (Fig. 3a), two markers of mitochondrial stress that are increased during the mitochondrial unfolded protein response [19]. Inhibition of CYPD using CsA reproduced the same effects (ESM Fig. 2a, b). Finally, the partial invalidation of CYPD expression by specific siRNA also induced ER stress markers (Fig. 3c).

NIM811 treatment also significantly reduced insulin-stimulated protein kinase B (PKB) phosphorylation (Fig. 3d) and induced *PEPCK* mRNA expression (ESM Fig. 2c) in HuH7 cells. Inhibition of CYPD using CsA reproduced all these effects (ESM Fig. 2d, e). In addition, the partial invalidation of CYPD expression by siRNA also altered insulin signalling (Fig. 3e) and induced *PEPCK* expression (ESM Fig. 2f). To strengthen the link between IP3R-mediated Ca^{2+} signalling, ER homeostasis and insulin signalling, we investigated whether pharmacological inhibition of IP3R could alter insulin signalling independently of CYPD. Both 2-APB and Xestospongin C treatments, which antagonise the calcium-releasing action of inositol-1,4,5-trisphosphate at the receptor

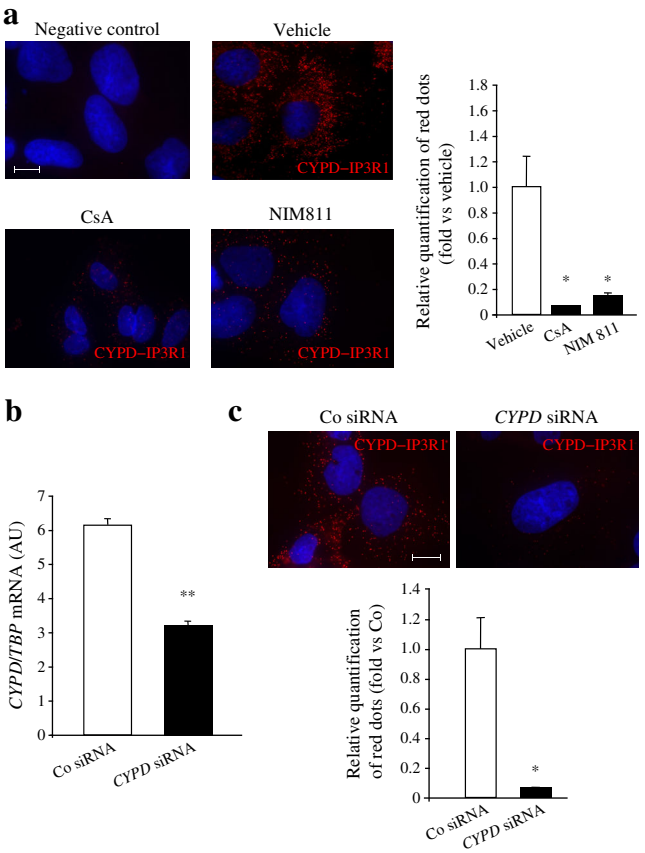

Fig. 1 Pharmacological and genetic inhibition of CYPD alters its interaction with the VDAC1–GRP75–IP3R1 complex. (**a**, **c**) Representative images (scale bar, 20 μm) and quantitative analysis of CYPD–IP3R1 interactions measured by in situ PLA in HuH7 cells, following treatment with either CsA or NIM811 (2 μmol/l, 16 h) (**a**), or silencing of *CYPD* (25 nmol/l, 48 h) (**c**). Nuclei appear in blue and PLA-specific signals in red. Magnification ×63. *$p<0.05$ vs control, $n=3$. Co, control. (**b**) Measurement of *CYPD* mRNA levels by real-time PCR in HuH7 cells silenced for *CYPD*. **$p<0.001$, $n=3$

level, significantly induced ER stress (Fig. 4a, b) and reduced insulin-stimulated PKB phosphorylation (Fig. 4c, d) in HuH7 cells.

Loss of CYPD in mice alters Ca^{2+} transfer from ER to mitochondria in isolated hepatocytes We previously found that ER–mitochondria interactions were reduced in liver of *CypD*-KO mice [10]. We confirmed in this study our initial observation using an independent group of mice (Fig. 5a) and further analysed the composition of MAM fractions of WT and *CypD*-KO mice. We found no significant modification of IP3R1, VDAC1, GRP75, mitofusin 2 (MFN2) or sarco(endo)plasmic reticulum Ca^{2+} ATPase 2 (SERCA2) protein level in MAM fractions of *CypD*-KO mice compared with WT mice (Fig. 5b). This suggests that loss of CYPD induces a dissociation of organelles rather than a change in MAM protein composition. We then examined inter-organelle Ca^{2+} flux in isolated hepatocytes of *CypD*-KO mice, following the same experimental protocol performed in HuH7 cells. In WT hepatocytes, histamine induced Ca^{2+} release from the ER, immediately followed by mitochondrial Ca^{2+} uptake (Fig. 5c, d). This histamine-stimulated Ca^{2+} transfer from the ER to mitochondria was completely abolished in *CypD*-KO hepatocytes (Fig. 5c, d). This occurs in the absence of a modification of *Serca2b* (also known as *Atp2a2*) and *Mcu* mRNA levels in liver of *CypD*-KO mice (ESM Fig. 3a). Together, these results confirm in a more physiological model that CYPD participates in IP3-mediated ER-to-mitochondria Ca^{2+} transfer in hepatocytes.

We also measured cytoplasmic Ca^{2+} in response to a discharge of ER store by thapsigargin, both in the presence and absence of extracellular Ca^{2+}. In both conditions, thapsigargin-sensitive Ca^{2+} stores were significantly higher in *CypD*-KO mice compared with WT mice (Fig. 5e, f),

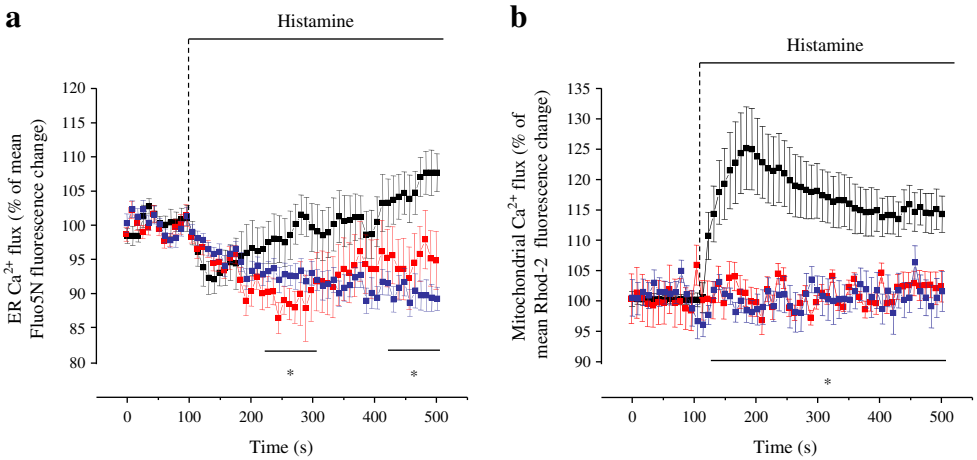

Fig. 2 Pharmacological and genetic inhibition of CYPD alters IP3R-mediated Ca^{2+} transfer between ER and mitochondria in HuH7 cells. (**a**, **b**) Measurement by confocal imaging of Ca^{2+} flux into ER (**a**) and mitochondria (**b**) in histamine-stimulated HuH7 cells, in control situation (Co, black curve), after NIM811 treatment (2 μmol/l, 16 h, red curve) or after siRNA-mediated *CYPD* silencing (25 nmol/l, 48 h, blue curve). Curves represent the time course of Ca^{2+} exchange between ER and mitochondria for 500 s after histamine stimulation (100 μmol/l), in the presence of extracellular Ca^{2+}. Mean Ca^{2+} flux was normalised to fluorescence values prior to histamine application. *$p<0.05$ vs control, $n=18$

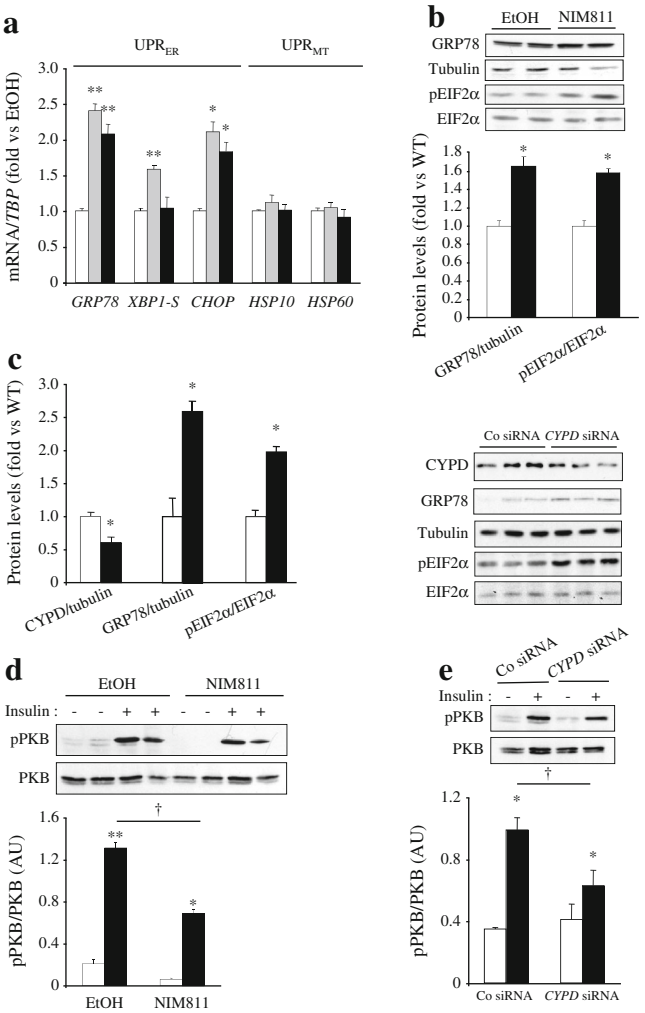

Fig. 3 Pharmacological and genetic inhibition of CYPD induces ER stress and alters insulin signalling in HuH7 cells. (**a**–**c**) Analysis of both mRNA (**a**) and protein levels (**b**, **c**) of ER stress markers in HuH7 cells following 6 (grey bars) or 16 (black bars) h of NIM811 treatment (**a**, **b**) or silencing of CYPD (**c**, black bars). UPR, unfolded protein response; MT mitochondria. (**d**, **e**) Analysis of PKB phosphorylation in basal situation (white bars) or after insulin stimulation (black bars) in HuH7 cells following NIM811 treatment (**d**) or *CYPD* silencing (**e**). Co, control. *$p<0.05$ and **$p<0.01$ vs Co; †$p<0.05$ vs vehicle, $n=3$

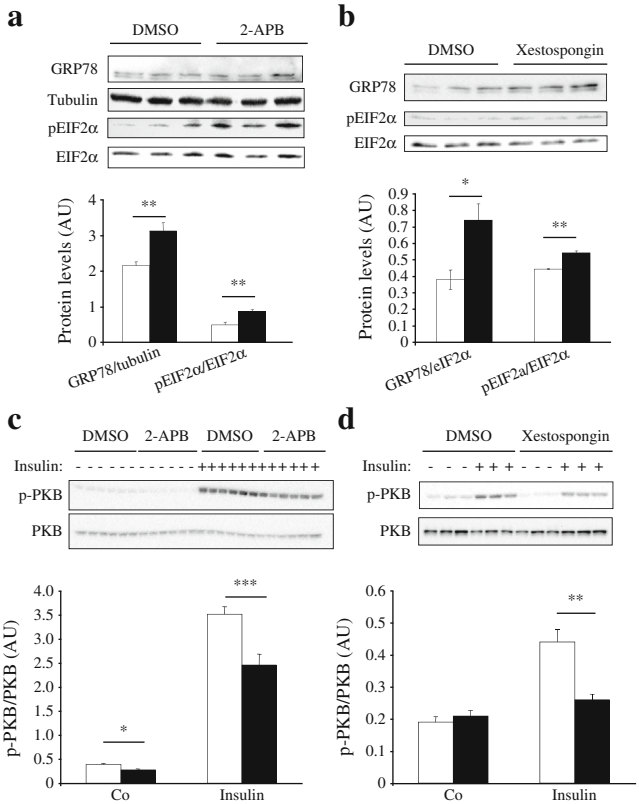

Fig. 4 Pharmacological inhibition of IP3R induces ER stress and alters insulin signalling in HuH7 cells. (**a**–**d**) Representative western blots and quantitative analysis of both ER stress markers (**a**, **b**) and insulin-stimulated PKB phosphorylation (**c**, **d**) in HuH7 cells treated (black bars) or not (white bars) with 2-APB (**a** and **c**, 50 μmol/l, 18 h) or Xestospongin (**b** and **d**, 1 μmol/l, 18 h). Co, control. *$p<0.05$, **$p<0.01$ and ***$p<0.005$, $n=3$–6

indicating that the reduced Ca^{2+} transfer from ER to mitochondria in *CypD*-KO hepatocytes was not due to a defect of ER Ca^{2+} storage. In addition, resting cytosolic Ca^{2+} was significantly increased in *CypD*-KO hepatocytes in the presence of extracellular Ca^{2+}, whereas this effect was absent in the absence of extracellular Ca^{2+} (ESM Fig. 3b, c). The cytosolic Ca^{2+} peak after histamine stimulation did not differ significantly between WT and *CypD*-KO mice, in either the presence or absence of extracellular Ca^{2+} (ESM Fig. 3d).

Loss of CYPD in mice induces ER stress and mitochondrial dysfunction in liver We then investigated ER or mitochondrial stress markers in the liver of WT and *CypD*-KO mice. We found increased mRNA levels of *Grp78* and *Chop* in the liver of *CypD*-KO mice, without any change in *Hsp10* and *Hsp60* expression (Fig. 6a). In addition, the phosphorylation of PERK, EIF2α and of JNK (a serine/threonine kinase involved in ER stress-induced hepatic insulin resistance [20]) was increased in liver of *CypD*-KO mice (Fig. 6b), confirming hepatic ER stress.

As Ca^{2+} import into mitochondria affects mitochondrial bioenergetics [21, 22], we studied mitochondrial respiration in either permeabilised (glutamate/malate) or intact (20 mmol/l glucose) primary hepatocytes of both WT and *CypD*-KO mice, in order to maintain ER mitochondria cross-talk. As shown in Fig. 6c, d, oxygen consumption was significantly reduced in *CypD*-KO hepatocytes, compared with WT hepatocytes.

Loss of CYPD in mice increases lipid accumulation and PKC activity and induces hepatic insulin resistance We previously reported that *CypD*-KO mice are glucose intolerant, insulin resistant and showed increased gluconeogenesis, based on tolerance tests [10]. Here, we further performed hyperinsulinaemic–euglycaemic clamp to confirm hepatic

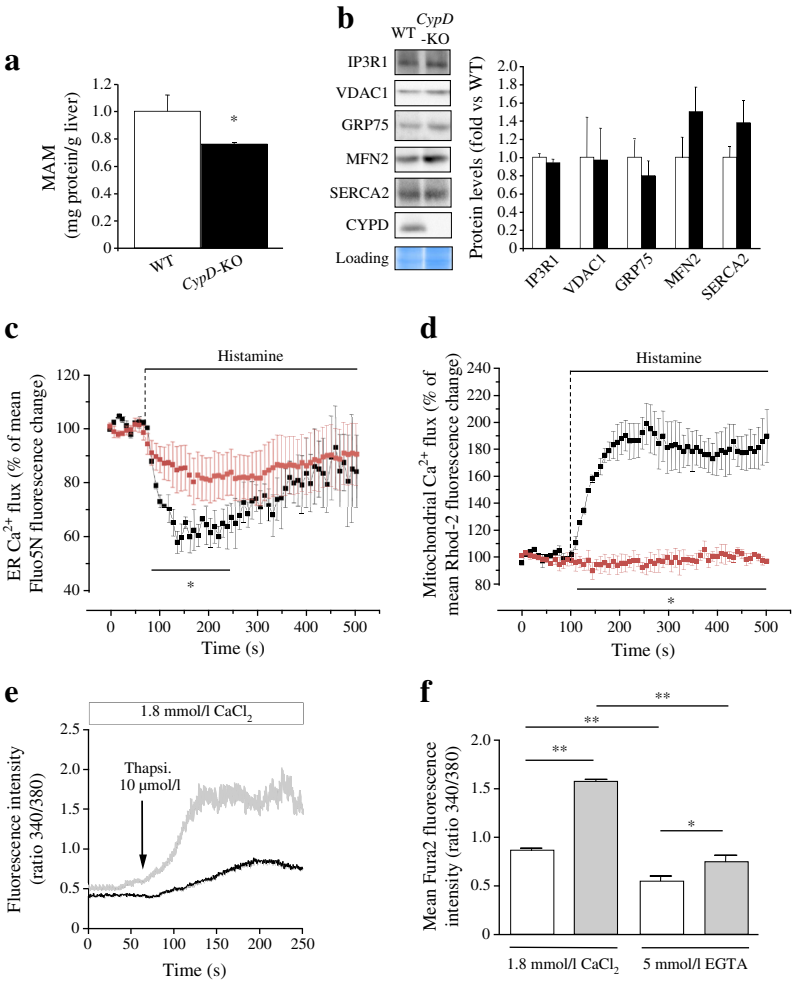

Fig. 5 Loss of CYPD alters IP3R-mediated Ca^{2+} transfer from ER to mitochondria in mouse hepatocytes. (**a**) Levels of MAM in liver of WT and *CypD*-KO mice, estimated by subcellular fractionation. *$p<0.05$ vs WT ($n=4$). (**b**) Representative western blots and quantitative analysis of proteins in hepatic MAM fractions of WT and *CypD*-KO mice ($n=4$). White bars, WT mice; black bars, *CypD*-KO mice. (**c**, **d**) Measurement of Ca^{2+} flux into ER (**c**) and mitochondria (**d**) in histamine-stimulated primary hepatocytes from WT (black curves) and *CypD*-KO (red curves) mice. Experiments and presentation of the results are as described in Fig. 2. *$p<0.05$ for *CypD*-KO vs WT ($n=12$). (**e**, **f**) Representative curves (**e**) and quantitative analysis (**f**) of cytosolic Ca^{2+} (Fura2), following depletion of ER Ca^{2+} storage by thapsigargin (Thapsi.; 10 μmol/l), in the presence (1.8 mmol/l $CaCl_2$) or absence (5 mmol/l EGTA) of extracellular Ca^{2+} in WT (black curve and white bars) and *CypD*-KO (grey curve and grey bars) mice. *$p<0.01$ and **$p<0.001$ for indicated comparisons ($n=16$–25)

insulin resistance. The glucose infusion rate required to maintain euglycaemia was significantly lower in *CypD*-KO mice compared with that in WT mice (Fig. 7a). In addition, the suppression of hepatic glucose production was significantly reduced in *CypD*-KO mice (Fig. 7b), whereas peripheral glucose utilisation was unaltered (Fig. 7a), indicating a specific state of hepatic insulin resistance. In agreement, the expression levels of gluconeogenic enzymes were increased in liver of *CypD*-KO mice (Fig. 7c).

We also examined lipid metabolism in both WT and *CypD*-KO mice. Circulating NEFA were not modified in *CypD*-KO mice compared with WT mice (0.19±0.05 vs 0.16±0.05 mmol/l, respectively, $n=10$), whereas blood TG levels were significantly increased (0.90±0.03 vs 0.60±0.05 g/l, respectively, $p<0.05$, $n=10$). Interestingly, the lipid staining (Fig. 7d), as well as TG and total DAG levels (Fig. 7e), were significantly increased in the liver of *CypD*-KO mice. As PKCε was shown to be involved in DAG-mediated hepatic insulin resistance [23], we analysed its activity by measuring its translocation from cytosol to membrane. Consistent with DAG accumulation, PKCε activity was induced in the livers of *CypD*-KO mice (Fig. 7f). Furthermore, the mRNA levels of genes related to β-oxidation (*Cpt1a*) were decreased in liver of *CypD*-KO mice, whereas the expression of both lipogenic genes (*Srebp1c* [also known as *Srebf1*], *Srebp1a*, *Fasn*, *Acaca*) and genes involved in lipid export (*Apob*, *Mttp*) were increased (Fig. 7g). The expression of neither *Mlycd* nor *Dgat2* was modified in liver of *CypD*-KO mice compared with WT mice. Altogether, these results suggest that lipid accumulation in liver of *CypD*-KO mice is likely related to both a

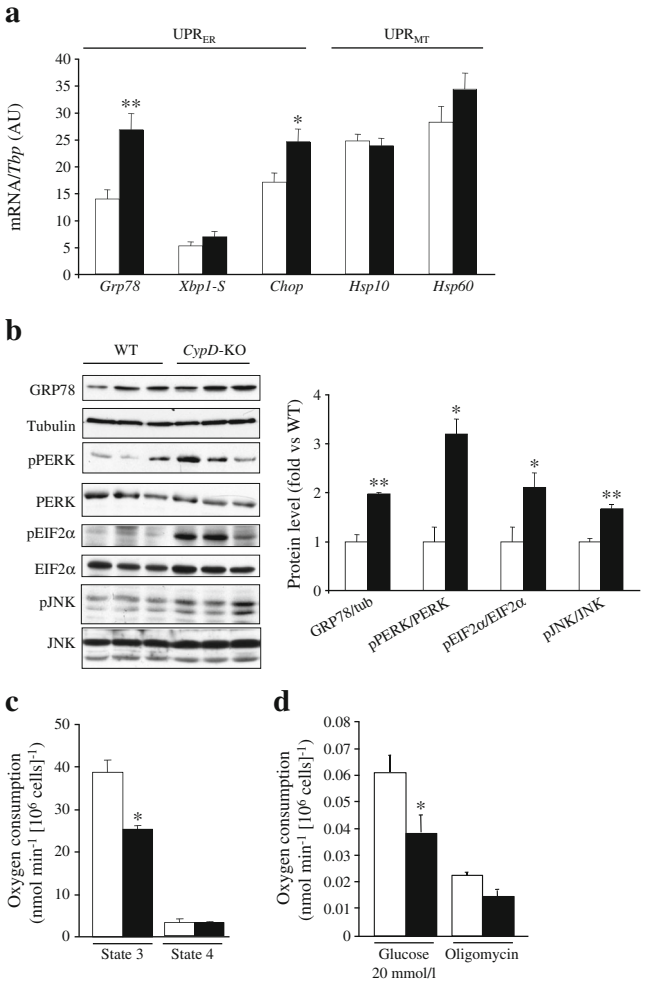

Fig. 6 Loss of CYPD induces hepatic ER stress and mitochondrial dysfunction in mice. (**a**, **b**) mRNA (**a**) and protein (**b**) levels of ER and mitochondria stress markers in liver of WT and *CypD*-KO mice. *$p<0.05$ and **$p<0.01$ vs WT mice ($n=3$–10). UPR, unfolded protein response; MT mitochondria; tub, tubulin. (**c**, **d**) Oxygen consumption measured in either permeabilised primary hepatocytes (**c**, in response to 5 mmol/l glutamate+25 mmol/l malate stimulation in both states 3 [+ 1 mmol/l ADP] and 4 [+ oligomycin]) or in intact hepatocytes (**d**, in the presence of 20 mmol/l glucose and after addition of oligomycin) from WT and *CypD*-KO mice. White bars, WT mice; black bars, *CypD*-KO mice. *$p<0.05$ vs WT ($n=4$)

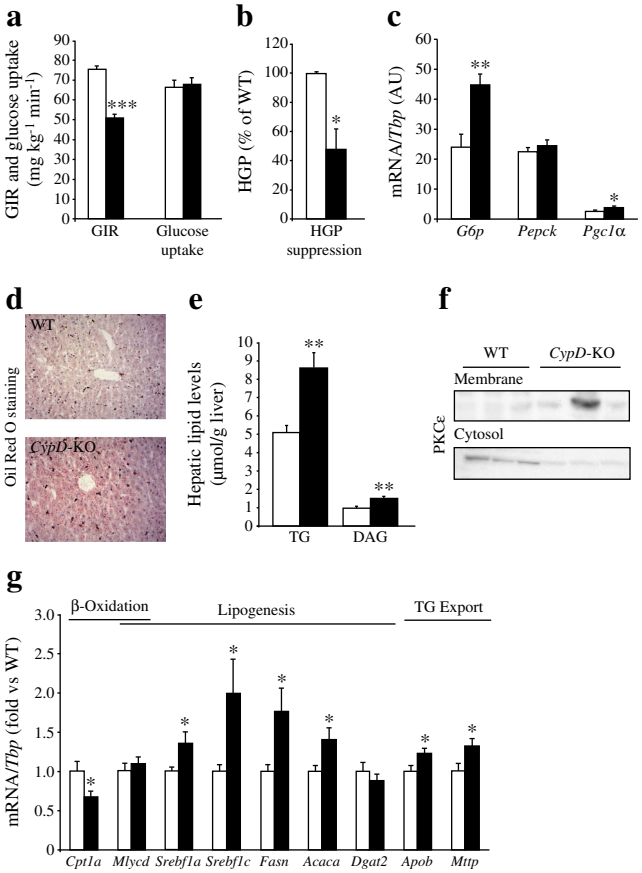

Fig. 7 Loss of CYPD induces hepatic insulin resistance and alterations of lipid homeostasis in mice. (**a**, **b**) Glucose infusion rate (GIR) and glucose uptake (**a**), as well as suppression of hepatic glucose production (HGP) (**b**) was measured under a hyperinsulinaemic–euglycaemic clamp in WT and *CypD*-KO mice ($n=4$). (**c**) Expression of gluconeogenic genes *G6p*, *Pepck* and *Pgc1α* (also known as *Ppargc1a*) in the liver of WT and *CypD*-KO mice ($n=10$). (**d**) Liver sections were stained with Oil Red O. Original magnification, ×20. (**e**) Hepatic TG and DAG content in liver of WT and *CypD*-KO mice ($n=6$). (**f**) Measurement of PKCε activation in cytosolic and membrane fractions of liver of WT and *CypD*-KO mice ($n=3$). (**g**) mRNA levels of genes related to β-oxidation, lipogenesis and TG export in liver of WT and *CypD*-KO mice ($n=10$). White bars, WT mice; black bars, *CypD*-KO mice. *$p<0.05$, **$p<0.01$ and ***$p<0.001$ vs WT

reduction in lipid oxidation and an increase in lipid storage, the latter being mainly associated with increased de novo lipogenesis.

Role of PKCε in CYPD-related alteration of insulin signalling Both JNK and PKCε enzymes, which are increased in liver of *CypD*-KO mice, are potential mediators of hepatic insulin resistance [20, 23]. To discriminate between the two, we measured the effect of CYPD silencing on insulin-stimulated PKB phosphorylation in the presence or absence of JNK and PKCε inhibitors. Inhibition of JNK with SP600125 did not modify *CYPD* siRNA-induced alteration of insulin-stimulated PKB phosphorylation (Fig. 8a), whereas inhibition of PKCε activity, using a specific peptide inhibitor of PKCε, prevented the reduction of insulin-stimulated PKB phosphorylation induced by CYPD silencing in HuH7 cells (Fig. 8b). Together, these data suggest a predominant role for PKCε, rather than JNK, in CYPD-related alterations of insulin signalling, at least in vitro.

Discussion

Hepatic insulin resistance is a principal component of type 2 diabetes, but the cellular and molecular mechanisms responsible for its pathogenesis are only partly known. We recently proposed a role for MAM integrity in the control of hepatic

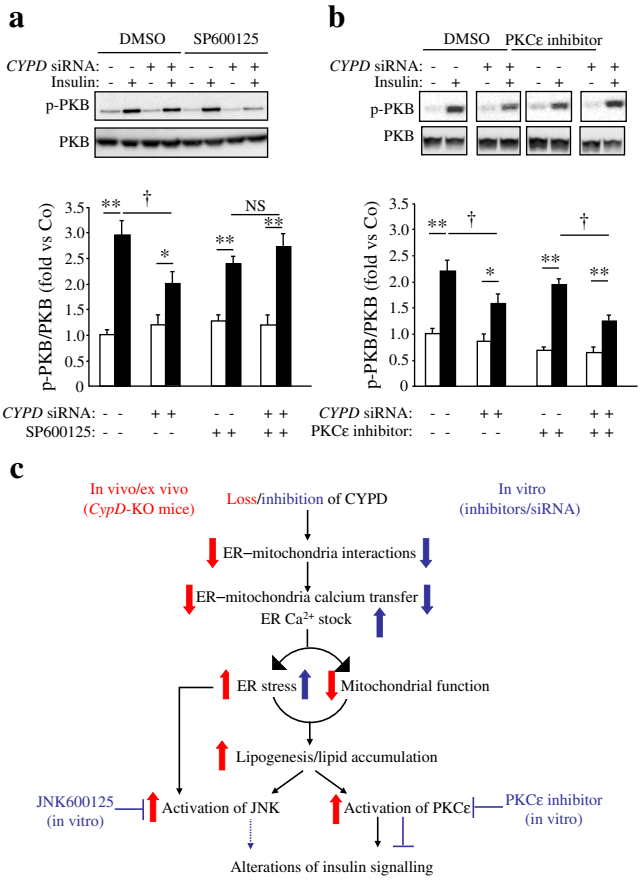

Fig. 8 Involvement of PKCε, but not of JNK, in *CYPD* siRNA-mediated alteration of insulin signalling in HuH7 cells. (**a**, **b**) Representative western blot and quantitative analysis of basal (white bars) and insulin-stimulated (black bars) PKB phosphorylation in HuH7 cells silenced for *CYPD*, in the presence or absence of an inhibitor of JNK (SP600125, 10 μmol/l) (**a**) or PKCε (specific peptide inhibitor of PKCε, 10 μmol/l) (**b**). For western blots shown in (**b**), four parts of the same gel are shown. *$p<0.05$ and **$p<0.01$ vs basal; $^{\dagger}p<0.05$ vs respective Co siRNA ($n=3$). (**c**) Schematic representation of the effects of loss/inhibition of CYPD on hepatic insulin resistance. Red, in vivo and ex vivo observations; blue, in vitro observations in HuH7 cells

insulin action and demonstrated that disruption of MAM integrity in the liver of *CypD*-KO mice can induce hepatic insulin resistance [10]. In the present study, we further investigated the underlying mechanisms and showed that the disruption of Ca^{2+} transfer from ER to mitochondria in the liver of *CypD*-KO mice is likely the molecular consequence of MAM disruption, accounting for defective insulin action in the liver.

ER–mitochondria contact points are known to be enriched in Ca^{2+}-handling proteins and chaperones and to generate microdomains with a high Ca^{2+} concentration [3]. We provide in vivo and in vitro evidence that pharmacological or genetic inhibition of the mitochondrial chaperone CYPD results in modifications of ER–mitochondria Ca^{2+} transfer: (1) via CYPD binding to the mitochondrial inner membrane since its actions are inhibited by CsA and NIM811 and (2) via an interaction with the VDAC1–GRP75–IP3R1 Ca^{2+}-channelling complex. These data are consistent with our recent study demonstrating that inhibition of CYPD in cardiomyocytes decreased the Ca^{2+} transfer from ER to mitochondria through IP3R under normoxic conditions [9]. Furthermore, CYPD-mediated disruption of ER–mitochondria cross-talk seems related rather to a dissociation of organelle than to a modification of protein expression at MAM interface, and seems independent of a modification of both *Mcu* and *Serca2b* mRNA levels. This new physiological role of CYPD in ER–mitochondria communication should now be considered as clinically relevant because inhibitors of CYPD function are either already used in clinical practice (e.g. CsA in transplanted patients) or are being developed (e.g. for treatment of hepatitis C virus or HIV infections) [24].

Our findings also point to a fundamental mechanism by which reduced structural and functional ER–mitochondria interactions alter organelle function and subsequently inhibit insulin's action, leading to hepatic insulin resistance. We thus propose a model by which the loss of CYPD can induce liver insulin resistance (Fig. 8c). Invalidation of CYPD alters ER–mitochondria interactions and Ca^{2+} exchange, leading to increased ER Ca^{2+} storage and ER stress. It is likely that the loss of CYPD-mediated uncoupling of the ER from the mitochondria is compensated by increased levels of the ER protein-folding machinery and Ca^{2+} to re-establish ER homeostasis, as previously reported [4, 5, 21]. At the same time, lack of Ca^{2+} transfer to mitochondria in *CypD*-KO mouse hepatocytes can reduce mitochondrial respiration, as also seen in a recent study demonstrating that constitutive low-level IP3R-mediated Ca^{2+} delivery to mitochondria is essential to maintain normal cellular bioenergetics [22]. The chronic disturbance of Ca^{2+} homeostasis likely maintains the activation of unfolded protein response in liver of *CypD*-KO mice, despite increased GRP78 expression. Subsequently, both ER stress and mitochondrial dysfunction may contribute to an increase in hepatic lipid levels. Indeed, fat accumulation in the liver of *CypD*-KO mice seems to be related to both a reduction in lipid oxidation (based on reduction in *Cpt1* expression) and an induction of de novo lipogenesis (based on induction of lipogenic genes), whereas esterification of lipid (based on the absence of change in circulating NEFA levels) and export of lipids (based on induction of *ApoB* and *Mttp* genes) from liver should not be altered. The induction of de novo lipogenesis is in agreement with the activation of both PERK and IRE1 branches of the unfolded protein response in the liver of *CypD*-KO mice, as both pathways were shown to activate the lipogenic transcription factor SREBP-1c [25–27]. Particularly, accumulation of DAG likely contributes to PKCε activation in the liver of *CypD*-KO mice. Together, these metabolic stresses would consequently result in alterations of hepatic insulin signalling and in the deterioration of glucose homeostasis in *CypD*-KO mice. Indeed, both induction of ER stress and accumulation of intracellular lipids have been involved in hepatic insulin resistance. Activation of JNK has been shown in ER stress-mediated hepatic insulin

resistance [20] and activation of PKCε has been related to DAG-induced hepatic insulin resistance [23]. In *CypD*-KO mice, hepatic insulin resistance appears to be mainly secondary to ER stress modulation of hepatic lipogenesis and subsequent DAG-mediated activation of PKCε rather than to ER stress-induced JNK activation, at least in vitro. Whereas an unspecific effect of inhibitors could not be excluded, this result fits well with the mechanisms recently proposed for another mouse model of insulin resistance [28], as well as with recent data in human liver [23]. Nevertheless, we cannot exclude the possibility that other players could be involved in the insulin-resistant phenotype of *CypD*-KO mice. Particularly, as absolute cytosolic Ca^{2+} levels were increased in *CypD*-KO mouse hepatocytes, we cannot exclude the participation of Ca^{2+}-sensitive kinases and/or phosphatases in the alteration of insulin signalling, as suggested by others studies [29, 30]. As disruption of MAM integrity has been observed in liver of different mouse models of obesity and type 2 diabetes [10], it is likely that the unexpected role of inter-organelle Ca^{2+} exchange in triggering hepatic insulin resistance might be extrapolated to these models. In agreement, the direct inhibition of IP3R, independently of CYPD, also induced ER stress and altered hepatic insulin signalling, suggesting that the proposed mechanism is a more general model and not restricted to the *CypD*-KO mouse model. Nevertheless, as controversy exists in this topic [31], further studies are required to clarify the role of inter-organelle Ca^{2+} exchange in triggering hepatic insulin resistance in obesity.

In conclusion, our data demonstrate that CYPD is an important regulator of MAM integrity and subsequently of Ca^{2+} exchange at the MAM interface, and provide the first evidence that IP3R-mediated Ca^{2+} transfer from ER to mitochondria is an essential cellular process involved in the control of hepatic insulin action. Therefore, modulation of ER–mitochondria Ca^{2+} exchange may provide an exciting new avenue for treating hepatic insulin resistance.

Acknowledgements The authors would like to thank the Lyon-Est imaging center (CIQLE) and SFR Santé Lyon Est (CNRS UMS3453 – INSERM US7, Université Lyon 1, France) for access to technological platforms and Physiogenex (Labege, France) for providing hyperinsulinaemic–euglycaemic clamps.

Funding This work was supported by Servier Laboratories, Inserm, the ANR (ANR-07-PHYSIO-020-01 and ANR-11-BSV1-033-02 from MO and ANR-09-JCJC-0116 from JR) and the FRM (MO, AL).

Duality of interest The authors declare that there is no duality of interested associated with this manuscript.

Contribution statement JR and MO conceived and designed the study. JF, MP, EBe, ET, MAC, AD, AB, GT, BB, MM, PT, GV, MD, EBl and LG contributed to the collection of data. JR, JF and MP analysed and interpreted the data. JR and MO wrote the paper. FZ, HV and AL contributed to study conception and reviewed the manuscript for important intellectual concept. All authors contributed to critical revisions and have read and approved the final version to be published. JR is responsible for the integrity of the work as a whole.

References

1. Giorgi C, De Stefani D, Bononi A, Rizzuto R, Pinton P (2009) Structural and functional link between the mitochondrial network and the endoplasmic reticulum. Int J Biochem Cell Biol 41:1817–1827
2. Szabadkai G, Bianchi K, Varnai P et al (2006) Chaperone-mediated coupling of endoplasmic reticulum and mitochondrial Ca^{2+} channels. J Cell Biol 175:901–911
3. Rizzuto R, Pinton P, Carrington W et al (1998) Close contacts with the endoplasmic reticulum as determinants of mitochondrial Ca^{2+} responses. Science 280:1763–1766
4. de Brito OM, Scorrano L (2008) Mitofusin 2 tethers endoplasmic reticulum to mitochondria. Nature 456:605–610
5. Simmen T, Aslan JE, Blagoveshchenskaya AD et al (2005) PACS-2 controls endoplasmic reticulum-mitochondria communication and Bid-mediated apoptosis. EMBO J 24:717–729
6. Csordas G, Renken C, Varnai P et al (2006) Structural and functional features and significance of the physical linkage between ER and mitochondria. J Cell Biol 174:915–921
7. van Vliet AR, Verfaillie T, Agostinis P (2014) New functions of mitochondria associated membranes in cellular signaling. Biochim Biophys Acta 1843:2253–2262
8. Woodfield K, Ruck A, Brdiczka D, Halestrap AP (1998) Direct demonstration of a specific interaction between cyclophilin-D and the adenine nucleotide translocase confirms their role in the mitochondrial permeability transition. Biochem J 336:287–290
9. Paillard M, Tubbs E, Thiebaut PA et al (2013) Depressing mitochondria-reticulum interactions protects cardiomyocytes from lethal hypoxia-reoxygenation injury. Circulation 128:1555–1565
10. Tubbs E, Theurey P, Vial G et al (2014) Mitochondria-associated endoplasmic reticulum membrane (MAM) integrity is required for insulin signaling and is implicated in hepatic insulin resistance. Diabetes 63:3279–3294
11. Betz C, Stracka D, Prescianotto-Baschong C, Frieden M, Demaurex N, Hall MN (2013) Feature article: mTOR complex 2-Akt signaling at mitochondria-associated endoplasmic reticulum membranes (MAM) regulates mitochondrial physiology. Proc Natl Acad Sci U S A 110:12526–12534
12. Sebastian D, Hernandez-Alvarez MI, Segales J et al (2012) Mitofusin 2 (Mfn2) links mitochondrial and endoplasmic reticulum function with insulin signaling and is essential for normal glucose homeostasis. Proc Natl Acad Sci U S A 109:5523–5528
13. Hagiwara A, Cornu M, Cybulski N et al (2012) Hepatic mTORC2 activates glycolysis and lipogenesis through Akt, glucokinase, and SREBP1c. Cell Metab 15:725–738
14. Ye R, Ni M, Wang M et al (2011) Inositol 1,4,5-trisphosphate receptor 1 mutation perturbs glucose homeostasis and enhances susceptibility to diet-induced diabetes. J Endocrinol 210:209–217
15. Schinzel AC, Takeuchi O, Huang Z et al (2005) Cyclophilin D is a component of mitochondrial permeability transition and mediates neuronal cell death after focal cerebral ischemia. Proc Natl Acad Sci U S A 102:12005–12010
16. Takahashi A, Camacho P, Lechleiter JD, Herman B (1999) Measurement of intracellular calcium. Physiol Rev 79:1089–1125
17. Berry MN, Friend DS (1969) High-yield preparation of isolated rat liver parenchymal cells: a biochemical and fine structural study. J Cell Biol 43:506–520

18. Nicolli A, Basso E, Petronilli V, Wenger RM, Bernardi P (1996) Interactions of cyclophilin with the mitochondrial inner membrane and regulation of the permeability transition pore, and cyclosporin A-sensitive channel. J Biol Chem 271:2185–2192
19. Zhao Q, Wang J, Levichkin IV, Stasinopoulos S, Ryan MT, Hoogenraad NJ (2002) A mitochondrial specific stress response in mammalian cells. EMBO J 21:4411–4419
20. Ozcan U, Cao Q, Yilmaz E et al (2004) Endoplasmic reticulum stress links obesity, insulin action, and type 2 diabetes. Science 306:457–461
21. Bravo R, Vicencio JM, Parra V et al (2011) Increased ER-mitochondrial coupling promotes mitochondrial respiration and bioenergetics during early phases of ER stress. J Cell Sci 124:2143–2152
22. Cardenas C, Miller RA, Smith I et al (2010) Essential regulation of cell bioenergetics by constitutive InsP3 receptor Ca2+ transfer to mitochondria. Cell 142:270–283
23. Kumashiro N, Erion DM, Zhang D et al (2011) Cellular mechanism of insulin resistance in nonalcoholic fatty liver disease. Proc Natl Acad Sci U S A 108:16381–16385
24. Quarato G, D'Aprile A, Gavillet B et al (2012) The cyclophilin inhibitor alisporivir prevents hepatitis C virus-mediated mitochondrial dysfunction. Hepatology 55:1333–1343
25. Li H, Min Q, Ouyang C et al (2014) AMPK activation prevents excess nutrient-induced hepatic lipid accumulation by inhibiting mTORC1 signaling and endoplasmic reticulum stress response. Biochim Biophys Acta 1842:1844–1854
26. Ning J, Hong T, Ward A et al (2011) Constitutive role for IRE1a-XBP1 signaling pathway in the insulin-mediated hepatic lipogenic program. Endocrinology 152:2247–2255
27. Zhang C, Chen X, Zhu RM et al (2012) Endoplasmic reticulum stress is involved in hepatic SREBP-1c activation and lipid accumulation in fructose-fed mice. Toxicol Lett 212:229–240
28. Jurczak MJ, Lee AH, Jornayvaz FR et al (2012) Dissociation of inositol-requiring enzyme (IRE1alpha)-mediated c-Jun N-terminal kinase activation from hepatic insulin resistance in conditional X-box-binding protein-1 (XBP1) knock-out mice. J Biol Chem 287:2558–2567
29. Ozcan L, Wong CC, Li G et al (2012) Calcium signaling through CaMKII regulates hepatic glucose production in fasting and obesity. Cell Metab 15:739–751
30. Wang Y, Li G, Goode J et al (2012) Inositol-1,4,5-trisphosphate receptor regulates hepatic gluconeogenesis in fasting and diabetes. Nature 485:128–132
31. Arruda AP, Pers BM, Parlakgül G et al (2014) Chronic enrichment of hepatic endoplasmic reticulum-mitochondria contact leads to mitochondrial dysfunction in obesity. Nat Med 20:1427–1435